Health Research Grant No. RR0317 from the Biotechnology Resources Branch, Division of Research Resources.

Registry No. $(\eta^5\text{-}C_5H_5)Fe(CO)_2Mn(CO)_5$, 12088-73-2; $(\eta^5\text{-}C_5Me_5)Fe(CO)_2Mn(CO)_5$, 95421-00-4; $(\eta^5\text{-}{}_5H_5)Fe(CO)_2Mn(CO)_4P(OPh)_3$, 108563-04-8; $[(\eta^5\text{-}C_5H_5)Fe(CO)_2]_2$, 12154-95-9; $[Mn(CO)_4P(OPh)_3]_2$, 15529-62-1; $(\eta^5\text{-}{}_5H_5)Fe(CO)_2Mn(CO)_4PPh_3$, 108563-05-9; $(\eta^5\text{-}C_5Me_5)Fe(CO)_2Mn(CO)_4PPh_3$, 108563-06-0; $[(\eta^5\text{-}C_5Me_5)Fe(CO)_2]_2$, 35344-11-7; $[Mn(CO)_5]_2$, 10170-69-1; $[Mn(CO)_4PPh_3]_2$, 10170-70-4; $ClMn(CO)_4PPh_3$, 14841-08-8; $ClMn(CO)_4P(OPh)_3$, 85362-16-9; $(\eta^5\text{-}C_5H_5)Fe(CO)_2Cl$, 12107-04-9; $(\eta^5\text{-}C_5H_5)Fe(CO)P(OPh)_3(Cl)$, 35025-27-5; $Mn(CO)_4(P(OPh)_3)Cl$, 85362-16-9; $(\eta^5\text{-}C_5H_5)FeMn(CO)_6$, 108563-07-1; $(\eta^5\text{-}C_5Me_5)FeMn(CO)_6$, 108563-08-2; $Mn(CO)_5Cl$, 14100-30-2; $Mn_2(CO)_{10}$, 10170-69-1.

Reactions of Ditungsten Hexaalkoxides with Alkynylplatinum(II) Complexes: Formation of Heterometallic Dicarbido Complexes in Competition with Products Derived from Alkyne Metathesis

Reed J. Blau, Malcolm H. Chisholm,* Kirsten Folting, and Ruji J. Wang

Contribution from the Department of Chemistry and Molecular Structure Center, Indiana University, Bloomington, Indiana 47405. *Received August 15, 1986*

Abstract: In hydrocarbon solutions *trans*-$Pt(C{\equiv}CH)_2(PMe_2Ph)_2$ (I) and $W_2(O\text{-}t\text{-}Bu)_6$ (II) react to give by successive eliminations of *t*-BuOH *trans*-$Pt(C{\equiv}CH)[C_2W_2(O\text{-}t\text{-}Bu)_5](PMe_2Ph)_2$ (III) and *trans*-$Pt[C_2W_2(O\text{-}t\text{-}Bu)_5]_2(PMe_2Ph)_2$ (IV). Compounds III and IV are shown to contain dicarbido(4−) ligands on the basis of ^{13}C NMR studies and single-crystal X-ray crystallography. The PtC_2W_2 units may also be classified as π-coordinated, dimetalla-substituted alkynes, $\{(\mu\text{-}PtC{\equiv}CW_\sigma){\equiv}W_\pi\}$. $(t\text{-}BuO)_3W{\equiv}CC{\equiv}W(O\text{-}t\text{-}Bu)_3$ (V) is also formed in the reaction between I with II. Its proposed mechanism of formation includes alkyne metathesis, trans to cis isomerization about Pt(II), and intramolecular reductive elimination from Pt(II). The complexes $(quin)(t\text{-}BuO)_3W{\equiv}CH$ and $Pt(PMe_2Ph)_4$ are formed in the reaction between I and II in the presence of excess quinuclidine and PMe_2Ph, respectively, supporting the proposed mechanism. I and $W_2(O\text{-}i\text{-}Pr)_6(py)_2$ (II′) yield products derived from alkyne metathesis, $W_2(O\text{-}i\text{-}Pr)_6(\mu\text{-}C_2H_2)(py)_2$, and dicarbide formation, *trans*-$Pt(C{\equiv}CH)[C_2W_2(O\text{-}i\text{-}Pr)_5](PMe_2Ph)_2$ (VI) and *cis*-$Pt[C_2W_2(O\text{-}i\text{-}Pr)_5](PMe_2Ph)_2$ (VII). VII, a cis complex, is unstable toward reductive elimination at ambient temperature, whereas IV, its bulkier trans analogue, is thermally stable to at least 75 °C. The reaction between II′ and *trans*-$Pt(C{\equiv}CMe)_2(PMe_2Ph)_2$ (I′) yields $W_3(\mu\text{-}O\text{-}i\text{-}Pr)_3(O\text{-}i\text{-}Pr)_6(\mu_3\text{-}CMe)$ as a product derived from $C{\equiv}C$ scission. The Pt-containing products formed in the reactions of both II′ with I and II′ with I′ are unstable toward reductive elimination, and $Pt(PMe_2Ph)_4$ is eventually formed. Phosphine exchange in IV is very slow relative to that in III or I because of the steric bulk of the two $-C_2W_2(O\text{-}t\text{-}Bu)_5$ ligands. Carbon monoxide adds across the $W{\equiv}W$ bonds of IV forming first *trans*-$Pt[C_2W_2(O\text{-}t\text{-}Bu)_5][C_2W_2(\mu\text{-}CO)(O\text{-}t\text{-}Bu)_5](PMe_2Ph)_2$ (VIII) and then *trans*-$Pt[C_2W_2(\mu\text{-}CO)(O\text{-}t\text{-}Bu)_5]_2(PMe_2Ph)_2$ (IX).

We are currently developing the organometallic chemistry of molybdenum and tungsten supported by alkoxide ligands with a view toward modeling the chemistry of the oxides of these elements.[1] Very few carbido clusters supported by alkoxide ligands are presently known,[2] especially when compared to the large variety and vast number of such clusters supported by carbonyl ligands.[3,4] Alkoxy ligands, which are strong π-donors, are clearly very different from the carbonyl ligand, a neutral π-acceptor. Because of this, the physical properties and reactivity of the carbido centers in the two types of clusters may be very different.

The reactions between $W_2(OR)_6(M{\equiv}M)$ compounds and alkynes have yielded a variety of products including terminal[5-9] and bridging (μ_2[10,11] and μ_3[12,13]) alkylidyne complexes, alkyne adducts,[13-15] and $\mu\text{-}C_4R'_4$-containing compounds.[16,17] We anticipated that reactions employing metal–alkynyl complexes would provide an entry into heterometallic carbido chemistry in which the heterometal atom(s) and alkoxide-supported tungsten(s) would be coordinated to either a C^{4-} or C_2^{x-} unit (x = 2, 3, 4, 5, or 6). Our initial efforts in this area were concentrated on reactions between *trans*-$Pt(C{\equiv}CH)_2(PMe_2Ph)_2$[18] (I) and $W_2(O\text{-}t\text{-}Bu)_6$[19] (II). The choice of reactants was based on the well-defined coordination chemistry of Pt(II) and the wealth of information that can be gleaned from coupling constants involving spin-active nuclei, ^{195}Pt, ^{13}C, ^{31}P, ^{183}W, and ^{1}H as shown below. Small

---

(1) Chisholm, M. H. *J. Solid State Chem.* **1985**, *57*, 120.

(2) Chisholm, M. H.; Folting, K.; Huffman, J. C.; Leonelli, J.; Marchant, N. S.; Smith, C. A.; Taylor, L. C. E. *J. Am. Chem. Soc.* **1985**, *107*, 3722.

(3) Bradley, J. S. *Adv. Organomet. Chem.* **1983**, *22*, 1.

(4) Tachikawa, M.; Muetterties, E. L. *Prog. Inorg. Chem.* **1981**, *28*, 203.

(5) Schrock, R. R.; Listemann, M. L.; Sturgeoff, L. G. *J. Am. Chem. Soc.* **1982**, *104*, 4291.

(6) Listemann, M. L.; Schrock, R. R. *Organometallics* **1985**, *4*, 75.

(7) Cotton, F. A.; Schwotzer, W.; Shamshoum, E. S. *Organometallics* **1984**, *3*, 1770.

(8) Chisholm, M. H.; Hoffman, D. M.; Huffman, J. C. *Inorg. Chem.* **1983**, *22*, 2903.

(9) Chisholm, M. H.; Conroy, B. K.; Huffman, J. C. *Organometallics* **1986**, *5*, 2384.

(10) Cotton, F. A.; Schwotzer, W.; Shamshoun, E. S. *Organometallics* **1983**, *2*, 1167.

(11) Cotton, F. A.; Schwotzer, W.; Shamshoun, E. S. *Organometallics* **1983**, *2*, 1340.

(12) Chisholm, M. H.; Folting, K.; Heppert, J. A.; Hoffman, D. M.; Huffman, J. C. *J. Am. Chem. Soc.* **1985**, *107*, 1234.

(13) Chisholm, M. H.; Conroy, B. K.; Folting, K.; Hoffman, D. M.; Huffman, J. C. *Organometallics* **1986**, *5*, 2457.

(14) Chisholm, M. H.; Folting, K.; Hoffman, D. M.; Huffman, J. C. *J. Am. Chem. Soc.* **1984**, *106*, 6794.

(15) Chisholm, M. H.; Conroy, B. K.; Huffman, J. C.; Marchant, N. S. *Angew. Chem. Int. Ed. Engl.* **1986**, *25*, 446.

(16) Chisholm, M. H.; Hoffman, D. M.; Huffman, J. C. *J. Am. Chem. Soc.* **1984**, *106*, 6806.

(17) Chisholm, M. H.; Hoffman, D. M.; Huffman, J. C. *Chem. Soc. Rev.* **1985**, *14*, 69.

(18) Bell, R. A.; Chisholm, M. H.; Couch, D. A.; Rankel, L. A. *Inorg. Chem.* **1977**, *16*, 677.

(19) Akiyama, M.; Chisholm, M. H.; Cotton, F. A.; Extine, M. W.; Haitko, D. A.; Little, D.; Fanwick, P. E. *Inorg. Chem.* **1979**, *18*, 2266.

0002-7863/87/1509-4552$01.50/0

Table I. Fractional Coordinates and Isotropic Thermal Parameters for the *trans*-Pt$[W_2C_2(O\text{-}t\text{-}Bu)_5]_2(PMe_2Ph)_2$ Molecule[a]

atom	10^4x	10^4y	10^4z	$10B_{iso}$, Å^2
Pt(1)	0.[b]	0[b]	0[b]	10
W(2)	310.5 (3)	−1976.3 (2)	−1403.7 (4)	12
W(3)	−1772.0 (4)	−3007.8 (2)	−2470.1 (4)	13
C(4)	−476 (9)	−1136 (6)	−1062 (10)	19
C(5)	−1433 (8)	−1822 (5)	−1697 (9)	11
P(6)	−958 (2)	−644 (1)	1434 (2)	14
C(7)	−786 (9)	−1620 (6)	1761 (10)	18
C(8)	−418 (10)	−101 (6)	3128 (10)	21
C(9)	−2654 (9)	−893 (6)	845 (10)	19
C(10)	−3422 (10)	−1560 (6)	−146 (11)	25
C(11)	−4689 (10)	−1752 (7)	−560 (13)	35
C(12)	−5228 (10)	−1301 (7)	−22 (13)	33
C(13)	−4462 (11)	−616 (8)	943 (12)	35
C(14)	−3166 (11)	−422 (7)	1391 (11)	28
O(15)	1288 (6)	−2280 (4)	117 (7)	21
C(16)	1405 (11)	−2976 (6)	810 (10)	23
C(17)	858 (11)	−3761 (7)	−181 (11)	32
C(18)	2796 (11)	−2786 (8)	1472 (13)	39
C(19)	786 (14)	−3015 (8)	1832 (14)	43
O(20)	1282 (6)	−1660 (4)	−2549 (6)	18
C(21)	1442 (10)	−2060 (6)	−3657 (10)	24
C(22)	324 (10)	−2155 (7)	−4909 (10)	23
C(23)	2628 (11)	−1493 (7)	−3807 (12)	32
C(24)	1592 (11)	−2867 (7)	−3317 (11)	27
O(25)	−2802 (6)	−2913 (4)	−4197 (7)	20
C(26)	−3408 (10)	−2413 (6)	−4994 (10)	22
C(27)	−2486 (10)	−1559 (7)	−4856 (11)	27
C(28)	−3898 (12)	−2841 (8)	−6452 (11)	36
C(29)	−4465 (10)	−2390 (7)	−4520 (13)	34
O(30)	−2122 (6)	−3350 (4)	−876 (6)	18
C(31)	−3166 (10)	−4020 (6)	−761 (10)	22
C(32)	−2800 (12)	−4768 (7)	−629 (13)	34
C(33)	−4335 (11)	−4124 (7)	−1938 (13)	33
C(34)	−3338 (12)	−3750 (7)	522 (12)	33
O(35)	−1603 (6)	−3956 (4)	−3218 (7)	20
C(36)	−1941 (11)	−4644 (6)	−4217 (11)	28
C(37)	−1116 (15)	−5155 (8)	−3672 (14)	56
C(38)	−1714 (12)	−4320 (7)	−5482 (12)	34
C(39)	−3341 (14)	−5112 (8)	−4598 (15)	53
C(40)	4602 (14)	10027 (10)	4375 (15)	52 (3)
C(41)	3712 (20)	9441 (14)	3323 (22)	25 (4)
C(41)	3470 (31)	9963 (21)	3533 (34)	57 (7)
C(42)	2880 (13)	9723 (8)	2112 (14)	43 (3)

[a] Isotropic values for those atoms refined anisotropically are calculated by using the formula given by: Hamilton, W. C. *Acta Crystallogr.* **1959**, *12*, 609. [b] Parameters marked by an asterisk (*) were not varied.

Table II. Selected Bond Distances (A) and Bond Angles (deg) for IV

Bond Distances			
Pt(1)–P(6)	2.293 (3)	Pt(1)–C(4)	2.050 (1)
W(2)–W(3)	2.445 (1)	W(2)–O(15)	1.883 (7)
W(2)–O(20)	1.907 (6)	W(2)–C(4)	2.052 (10)
W(2)–C(5)	2.121 (8)	W(3)–O(25)	1.912 (7)
W(3)–O(30)	1.930 (6)	W(3)–O(35)	1.897 (6)
W(3)–C(5)	2.054 (9)	P(6)–C(7)	1.809 (10)
P(6)–C(8)	1.812 (g)	P(6)–C(9)	1.830 (10)
O(15)–C(16)	1.463 (12)	O(20)–C(21)	1.433 (11)
O(25)–C(26)	1.443 (12)	O(30)–C(31)	1.454 (12)
O(35)–C(36)	1.429 (12)	C(4)–C(5)	1.336 (13)
Bond Angles			
P(6)–Pt(1)–P(6′)	180.0	P(6)–Pt(1)–C(4)	92.2 (3)
C(4)–Pt(1)–C(4′)	180.0	W(3)–W(2)–O(15)	113.1 (2)
W(3)–W(2)–O(20)	115.6 (2)	W(3)–W(2)–C(4)	90.2 (3)
W(3)–W(2)–C(5)	52.9 (2)	O(15)–W(2)–O(20)	107.6 (3)
O(15)–W(2)–C(4)	117.0 (3)	O(15)–W(2)–C(5)	127.3 (3)
O(20)–W(2)–C(4)	112.9 (3)	O(20)–W(2)–C(5)	124.4 (3)
C(4)–W(2)–C(5)	37.3 (4)	W(2)–W(3)–O(25)	119.7 (2)
W(2)–W(3)–O(30)	99.1 (2)	W(2)–W(3)–O(35)	108.7 (2)
W(2)–W(3)–C(5)	55.4 (2)	O(25)–W(3)–O(30)	133.1 (3)
O(25)–W(3)–O(35)	90.6 (3)	O(25)–W(3)–C(5)	92.6 (3)
O(30)–W(3)–O(35)	101.5 (3)	O(30)–W(3)–C(5)	88.5 (3)
O(35)–W(3)–C(5)	162.8 (3)	Pt(1)–Pt(6)–C(7)	115.6 (3)
Pt(1)–P(6)–C(8)	116.3 (3)	Pt(1)–P(6)–C(9)	114.1 (3)
C(7)–P(6)–C(8)	101.2 (5)	C(7)–P(6)–C(9)	103.1 (4)
C(8)–P(6)–C(9)	104.7 (5)	W(2)–O(15)–C(16)	143.8 (6)
W(2)–O(20)–C(21)	136.0 (6)	W(3)–O(25)–C(26)	146.6 (6)
W(3)–O(30)–C(31)	129.2 (6)	W(3)–O(35)–C(36)	154.9 (7)
Pt(1)–C(4)–W(2)	140.8 (5)	Pt(1)–C(4)–C(5)	143.9 (8)
W(2)–C(4)–C(5)	74.2 (6)	W(2)–C(5)–W(3)	71.7 (3)
W(2)–C(5)–C(4)	68.5 (6)	W(3)–C(5)–C(4)	140.2 (7)

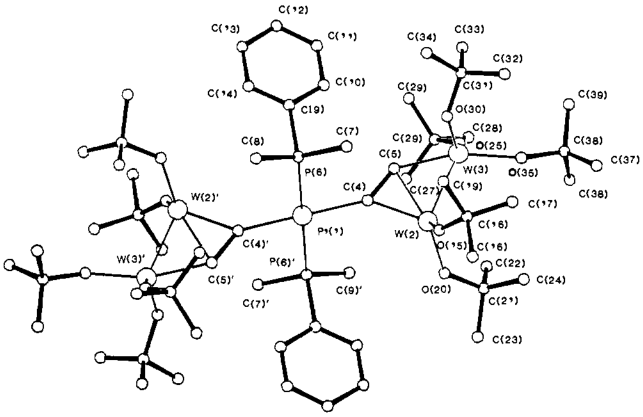

Figure 1. A ball and stick drawing of the *trans*-Pt$(PMe_2Ph)_2\{C_2W_2(O\text{-}t\text{-}Bu)_2\}_2$ molecule giving the atom numbering scheme used in the tables.

changes in the reactants, *i*-PrO vs. *t*-BuO and propynyl vs. ethynyl, altered the course of the reactions. Evidence for two types of reactions are described: C≡C cleavage (eq 1a) and, for R′ = H, a proton transfer from the ethynyl to an alkoxide ligand yielding a dicarbido ligand and alcohol (eq 1b). A preliminary finding was reported previously.[20]

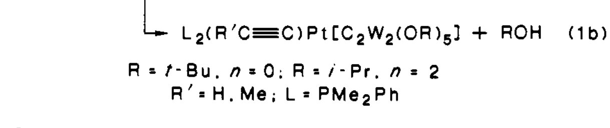

$$W_2(OR)_6(py)_n + Pt(C{\equiv}CR')_2L_2 \rightarrow (RO)_3W{\equiv}CR' + L_2(R'C{\equiv}C)PtC{\equiv}W(OR)_3 \quad (1a)$$

$$W_2(OR)_6(py)_n + Pt(C{\equiv}CR')_2L_2 \rightarrow L_2(R'C{\equiv}C)Pt[C_2W_2(OR)_5] + ROH \quad (1b)$$

R = *t*-Bu, *n* = 0; R = *i*-Pr, *n* = 2
R′ = H, Me; L = PMe_2Ph

Results and Discussion

Reaction of *trans*-Pt(C≡CH)$_2$(PMe$_2$Ph)$_2$ with W$_2$(O-*t*-Bu)$_6$. This reaction has been monitored by ^1H, ^{13}C, and ^{31}P NMR spectroscopy. It proceeds very slowly, 5–6 days at 30 °C in toluene, yielding three observable metal-containing products. Two of these products, *trans*-Pt$(C{\equiv}CH)[C_2W_2(O\text{-}t\text{-}Bu)_5](PMe_2Ph)_2$ (III) and *trans*-Pt$[C_2W_2(O\text{-}t\text{-}Bu)_5]_2(PMe_2Ph)_2$ (IV), are formed by two sequential "acid/base" reactions (eq 1b) yielding *t*-BuOH as an observable byproduct. The third, $(t\text{-}BuO)_3W{\equiv}CC{\equiv}W(O\text{-}t\text{-}Bu)_3$ (V), is formed parallel to III. When the stoichiometry of the reaction is 2:1 for II:I respectively, IV constitutes 75–85% of the final products with the remainder being V. A 1:1 stoichiometry yields mixtures of III and IV (and V) suggesting that the two sequential acid/base reactions occur at comparable rates. The reaction was also followed between the ^{13}C-labeled ethynyl compound *trans*-Pt$(^*C{\equiv}^*CH)_2(PMe_2Ph)_2$ (I*) which exists in a variety of isotopomers resulting from its preparation employing commercially available (Merk, Sharp, and Dohme) H*C≡*CH, where *C represents 92% g atom ^{13}C. In these reactions the labeled ^{13}C compounds III*, IV*, and V* are formed.

Crystal Structure of *trans*-Pt[C$_2$W$_2$(O-*t*-Bu)$_5$]$_2$(PMe$_2$Ph)$_2$] (IV) and the Properties of Its C$_2$$^{4-}$ Units. Fractional coordinates and isotropic thermal parameters are given in Table I. Pertinent bond distances and angles are found in Table II. The molecular structure of IV is centrosymmetric and is shown in Figure 1. A ball and stick view of the central $PtP_2(C_2W_2O_5)_2$ skeleton is shown in Figure 2. The central PtP_2C_2 unit is essentially square-planar,

---

(20) Blau, R. J.; Chisholm, M. H.; Folting, K.; Wang, R. J. *J. Chem. Soc., Chem. Commun.* **1985**, 1582.

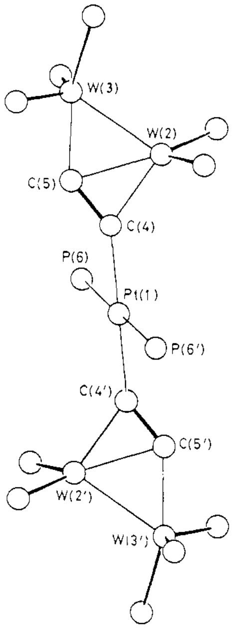

Figure 2. A ball and stick view of the central *trans*-$PtP_2(C_2W_2O_5)_2$ moiety of the centrosymmetric *trans*-$Pt(PMe_2Ph)_2\{C_2W_2(O\text{-}t\text{-}Bu)_5\}_2$ molecule looking nearly down the P–Pt–P axis showing the planar Pt-C_2W_2 unit.

Table III. NMR Chemical Shifts (ppm) and Coupling Constants (Hz) for *trans*-$Pt(C{\equiv}CH)_2(PMe_2Ph)_2$ and Derivatives Formed from Its Reactions with $W_2(OR)_6(py)_n$ (R = *t*-Bu, $n = 0$; R = *i*-Pr, $n = 2$)[a]

constant	I	III	IV	VI	VII
$\delta(P)$	−14.7	−11.2	−8.0	−7.6	−3.7
$^1J(^{195}Pt-^{31}P)$	2447	2591	2776	2757	3171
$\delta(C_\alpha)$	100.7	100.5	na	94–100	na
$^1J(^{195}Pt-^{13}C_\alpha)$	947	941	na	nd	na
$\delta(C_1)$	na	235.2	233.9	227.8	216.9
$^1J(^{195}Pt-^{13}C_1)$	na	802	801	814	983
$\delta(C_\beta)$	94.9	97.1	na	94–100	na
$^2J(^{195}Pt-^{13}C_\beta)$	266	259	na	nd	na
$\delta(C_2)$	na	302.1	302.0	284.3	282.3
$^2J(^{195}Pt-^{13}C_2)$	na	78	76	86	115
$^1J(^{183}W-^{13}C_2)$	na	132	133	nd	nd
$^1J(C_\alpha-C_\beta)$	122	122	na	122	na
$^1J(C_1-C_2)$	na	19	~19	nd	~19
$^2J(CPtC)$	40	36	39	nd	nd

[a] Notations for carbon atoms are as follows: $Pt{-}C_\alpha{\equiv}C_\beta H$ and $Pt{-}\{C_1{=}C_2W_2(OR)_5\}$; na = not applicable; nd = not determined.

and the bond distances and coupling constants to ^{195}Pt (Table III) establish this as formally Pt^{2+}. The $(W_2C_2)Pt(C_2W_2)'$ unit is also planar, and it forms a 62° angle with the PtP_2C_2 plane. This deviation from 90° minimizes steric crowding between the PMe_2Ph phenyls and the *tert*-butoxy methyls. The Pt(1)–C(4) and W(3)–C(5) distances in IV may be taken to represent Pt–C and W–C single bond distances and the C(4)–C(5) distance, 1.33 (1) Å, and W(2)–W(3) distance, 2.445 (1) Å, as C–C[21] and W–W[22] double bond distances, respectively. This allows the formal electron counting of each W as W(4+) and the C_2 units as C_2^{4-}.

The C_2 units in IV may be classed as either dimetalla-substituted alkynes and thus related to normal alkynes in their modes of binding to transition metals, or they may also be described as peripheral dicarbido units, C_2^{4-}, in a heterometallic cluster. Thus, comparisons with other dicarbido clusters prove useful.

Chart I. Structural Comparisons of Coordinated Alkynes Having Substituents in a Trans Configuration

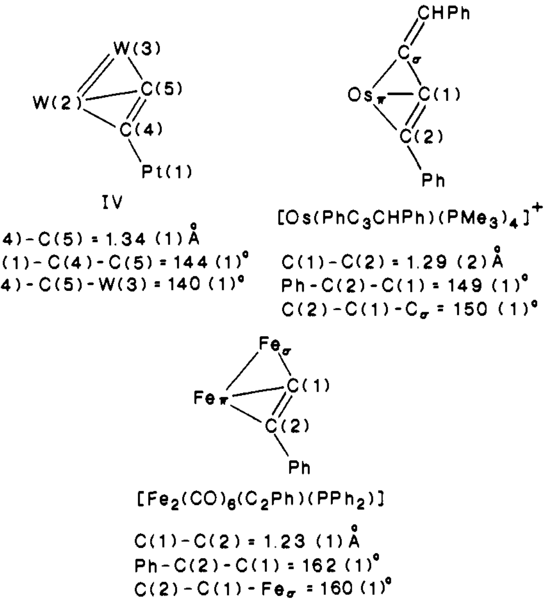

IV

C(4)–C(5) = 1.34 (1) Å
Pt(1)–C(4)–C(5) = 144 (1)°
C(4)–C(5)–W(3) = 140 (1)°

$[Os(PhC_3CHPh)(PMe_3)_4]^+$

C(1)–C(2) = 1.29 (2) Å
Ph–C(2)–C(1) = 149 (1)°
C(2)–C(1)–C_σ = 150 (1)°

$[Fe_2(CO)_6(C_2Ph)(PPh_2)]$

C(1)–C(2) = 1.23 (1) Å
Ph–C(2)–C(1) = 162 (1)°
C(2)–C(1)–Fe_σ = 160 (1)°

Pt(1) and W(3) are bound to the C_2 unit in IV through σ bonds forming a dimetalla-substituted alkyne which, in addition, is bound in a π fashion to W(2). This bonding mode is very similar to that found for the monometalla-substituted alkyne or acetylide unit in $Fe_2(CO)_6(\eta^2\text{-}\mu\text{-}C{\equiv}CPh)(\mu\text{-}PPh_2)$[23] and those in other related binuclear acetylides, $M_2(CO)_4(L)_2(\eta^2\text{-}\mu\text{-}C{\equiv}CR)(\mu\text{-}PPh_2)$, where M = Fe or Ru and R = alkyl or aryl.[24,25] As opposed to normal alkynes, $R{-}C{\equiv}C{-}R'$, where, upon coordination to a transition metal, the R and R′ substituents bend away from the metal in a cis configuration relative to each other; in IV, W(3) and Pt(1) are found in a trans configuration (see Chart I). Such is also the case for the Fe_σ and Ph substituents on the $C{\equiv}C$ unit of $Fe_2(CO)_6(\eta^2\text{-}\mu\text{-}C{\equiv}CPh)(\mu\text{-}PPh_2)$ in Chart I. The trans configuration of the substituents in IV and $Fe_2(CO)_6(\eta^2\text{-}\mu\text{-}C{\equiv}CPh)(\mu\text{-}PPh_2)$ is caused by an interaction between W(3) and W(2) in the former and Fe_σ and Fe_π in the latter in addition to the normal M_π to $C{\equiv}C$ π-interactions observed for normal alkynes. A similar trans configuration of substituents about a transition-metal-bound alkyne is observed in $[Os(\eta^3\text{-}PhC{\equiv}CC{=}CHPh)(PMe_3)_4]^+$.[26] In this case, the substituent bound to M_π is C_σ instead of M_σ.

The coordination of normal alkynes gives rise to the lengthening of the C–C bond in addition to the bending of the C–R bonds away from the metal complex as was mentioned above. Both effects depend mainly on the π-back-donation from metal orbitals to an antibonding MO of the alkyne and can be taken as a measure of the reduction of triple-bond character upon coordination. In fact, a plot of C–C–R angles vs. length of the C–C bond has shown a good correlation between the two in a wide variety of coordinated alkynes.[27] We report a similar trend in coordinated alkynes having trans-related substituents: as the C–C bond distances increase toward that of a double bond, the C–C–S (S = substrate) angles become less obtuse. In fact, the data listed in Chart I for IV, the Os complex, and the Fe_2 dimer fit very well into the plot compiled by Gervasio et al.[27] and span the range of C–C bond lengths and C–C–R bond angles observed for mononuclear complexes of the η^2-type. When compared to C–C bond distances in alkyne complexes of ditungsten alkoxides, the C(4)–C(5) bond distance in IV, 1.34 (1) Å, is intermediate between that of η^2-alkynes, 1.29 (2)[16] and 1.31 (1) Å,[28] and the μ-perpendicular-type, 1.374 (15) Å.[14] However, the C–C–S angles for both the η^2- and μ-per-

---

(21) Kutchitsu, K. *J. Chem. Phys.* **1966**, *44*, 906.

(22) Chisholm, M. H. *Polyhedron* **1983**, *2*, 681.

(23) Patel, H. A.; Fischer, R. G.; Carty, A. J.; Naik, D. V.; Palenik, G. J. *J. Organomet. Chem.* **1973**, *60*, C49.

(24) Carty, A. *J. Pure Appl. Chem.* **1973**, *54*, 113.

(25) Smith, W. F.; Yule, J.; Taylor, N. J.; Paik, H. N.; Carty, A. J. *Inorg. Chem.* **1977**, *16*, 1593.

(26) Gotzig, J.; Otto, H.; Werner, H. *J. Organomet. Chem.* **1985**, *287*, 247.

(27) Gervasio, G.; Rossetti, R.; Stanghellini, P. L. *Organometallics* **1985**, *4*, 1612.

(28) Chisholm, M. H.; Eichhorn, B. W.; Huffman, J. C. *J. Chem. Soc., Chem. Commun.* **1985**, 861.

Table IV. Elemental Analysis of *trans*-$Pt(C_2W_2(O\text{-}t\text{-}Bu)_5)_2(PMe_2Ph)_2$ ($C_{80}H_{112}P_2PtO_{10}W_4$)

	C	H	P
calcd	36.29	5.68	3.12
obsd	33.94	5.50	3.10
C_{56} + 4 WC[a]	33.87	5.68	3.10

[a] This calculated elemental analysis assumes that only 56 of the total 60 carbons in IV are combustible and that the remaining four form tungsten carbide.

pendicular alkynes, 136 (3)°[16,28] and 133 (1)°,[14] respectively, are less obtuse than those seen for IV, 142 (3)°. The C_2 units in IV may very well be classified as dimetalla-substituted alkynes bound in an η^2-fashion to an additional metal center.

The C_2 unit in IV may also be classed as a peripheral[4] dicarbido ligand, C_2^{4-}.[27] Metal clusters containing such moieties are very rare at present with $[Co_6(\mu_6\text{-}C_2)(\mu\text{-}CO)_6(CO)_8(\mu_4\text{-}S)]$, C–C = 1.37 (2) Å,[29] being the only other reported example. In most dicarbido clusters where the two carbon atoms are within bonding distance, the C_2 unit is encapsulated in a metal polyhedron.[29,30] The C–C bond distances in these caged clusters are fairly long ranging from 1.38 Å[30] in $[Ni_{16}(CO)_{23}(C_2)_2]^{4-}$ to 1.66 (6) Å[31] in $[Co_{11}(C_2)(CO)_{22}]$. The bond distance in IV, 1.34 Å, is shorter than all examples of dicarbido units listed above. This is due in part to bonding with fewer metals.[32]

One piece of evidence supporting the strong W–C interactions in the W_2C_2 units in IV comes from its elemental analysis which is listed in Table IV. Although the analyses for H and P are reasonable, the analysis for C is four carbons short (see Table IV). A plausible explanation for this discrepancy is that the four carbons in the C_2W_2 units form 4 equiv of tungsten carbide upon combustion consistent with their carbidic nature in IV.

The ^{13}C NMR Characterization of I*, III*, and IV*. Although *trans*-$Pt(C{\equiv}CH)\{C_2W_2(O\text{-}t\text{-}Bu)_5\}(PMe_2Ph)_2$ (III) was not isolated as a pure crystalline solid, it is well-characterized by NMR techniques. III* has ^{13}C resonances at 100.5 and 97.1 ppm similar to those corresponding to the C≡CH ligands in I* at 100.7 and 94.9 ppm, respectively. It also has ^{13}C resonances at 235.2 and 302.1 ppm similar to those attributed to the C_2 units in IV* at 233.9 and 302.0 ppm, respectively. In addition, the $^{195}Pt\text{–}^{13}C$, $^{183}W\text{–}^{13}C$, and $^{13}C\text{–}^{13}C$ coupling constants observed for the C≡CH ligand in I* and the C_2 unit in IV* parallel those observed for the corresponding C_2 units in III* (see Table III).

The coupling patterns for the ^{13}C-labeled resonances of I* in Figure 3, III*, and IV*[20] are very complex. When only $^{13}C\text{–}^{13}C$ couplings for the major isotopomer in each complex* are considered, AA′BB′, ABMX, and AA′XX′ coupling patterns are observed for I*, III*, and IV*, respectively. In addition, every line in each of these C_4 patterns is split into a triplet by the two equivalent ^{31}P nuclei. What adds further to the complexity of these spectra is the fact that the major isotopomer $^{13}C_4$ is found in 47% abundance in I*, and only 26% abundance in IV*. ^{195}Pt satellites, ^{183}W satellites for III* and IV*, and resonances due to the various isotopomers $^{13}C_3$ are also observed. Despite their inherent complexity, the various resonances were simulated, e.g., I* in Figure 3, and the coupling constants were determined (Table III).

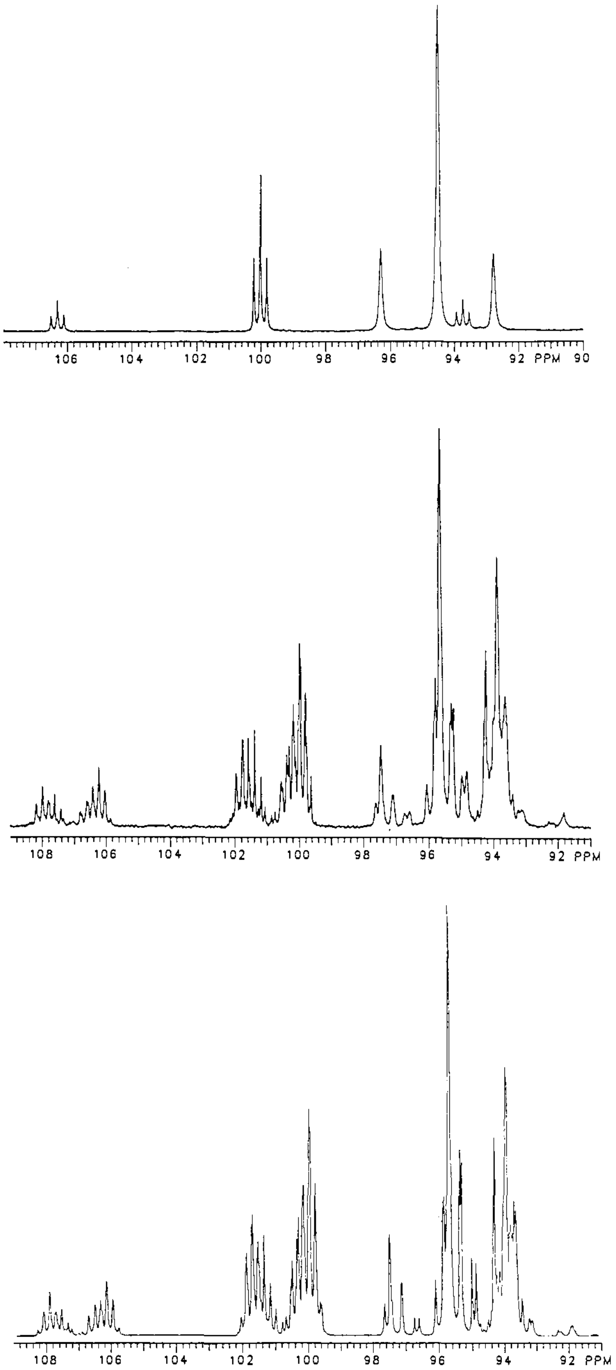

Figure 3. The ^{13}C NMR spectrum of the $-C{\equiv}CH$ resonances of *trans*-$Pt(C{\equiv}CH)_2(PMe_2Ph)_2$ with ^{13}C at natural abundance (top) and with a 92% g atom ^{13}C label at both acetylide carbon positions (middle). A spectral simulation of the latter (bottom) is also shown.

Perhaps more noteworthy among the various coupling constants for I*, III*, and IV* are the $^1J(^{13}C\text{–}^{13}C)$ values listed in Table III. For the Pt—C≡CH moiety, the values are 122 Hz whereas those for the PtW_2C_2 unit are very small 18–19 Hz. For comparison, $^1J(^{13}C\text{–}^{13}C)$ in ethyne, ethylene, and ethane are 171.5, 67.6, and 34.6 Hz, respectively. The low value of $J(^{13}C\text{–}^{13}C)$ in the PtC_2W_2 unit is similar to values seen for $W_2(\mu\text{-}C_2R_2)$-containing compounds supported by alkoxide ligands where the central W_2C_2 unit is best described as a dimetallatetrahedrane.[17] Apparently, bonding of such C_2 units to the tungsten centers dramatically reduces the "s" character of the C–C bond. Other couplings through the C–C bond of the PtC_2W_2 unit are also reduced significantly relative to those observed for the Pt—C≡CH moiety, e.g., $^2J(^{195}Pt\text{–}^{13}C_\beta)$ = 259 Hz in I* vs. $^2J(^{195}Pt\text{–}^{13}C_2)$ = 78 Hz in III*.

$[(t\text{-}BuO)_3W{\equiv}C]_2$ (V) and Its Mechanism of Formation. One complex formed from the reaction of I and II was found to contain no platinum. There is evidence that it is $[(t\text{-}BuO)_3W{\equiv}CC{\equiv}W\text{-}$

---

(29) Gervasio, G.; Rossetti, R.; Stanghellini, P. L.; Bor, G. *Inorg. Chem.* **1983**, *23*, 2073 and references therein.

(30) (a) Ceriotti, A.; Longoni, G.; Manassero, M.; Masciocchi, N.; Giampiero, P.; Resconi, L.; Sansoni, M. *J. Chem. Soc., Chem. Commun.* **1985**, 1402. (b) Arrigoni, A.; Ceriotti, A.; Pergola, R. D.; Longini, G.; Manassero, M.; Sansoni, M. *J. Organomet. Chem.* **1985**, *296*, 243. (c) Ceriotti, A.; Longoni, G.; Manassero, M.; Masciocchi, N.; Resconi, L.; Sansoni, M. *J. Chem. Soc., Chem. Commun.* **1985**, 181. (d) Arrigoni, A.; Ceriotti, A.; Pergola, R. D.; Longini, G.; Manassero, M.; Masciocchi, N.; Sansoni, M. *Angew. Chem., Int. Ed. Engl.* **1984**, *23*, 322.

(31) Albano, V. G.; Braga, D.; Ciani, G.; Martinengo, S. *J. Organomet. Chem.* **1982**, *213*, 293.

(32) See ref 27: the number of metal atoms to which an alkyne is bonded is one of the most important factors determining its C–C bond length.

Table V. Major ^{13}C NMR-Active Isotopomers in V*, 50:50 V:V*, and 50:50 V:V* Scrambled

isotopomer	% in V*	% in 50:50 V:V	% in scrambled 50:50 V:V*
W*C*CW	62	31	16
W*CCW	11	5	37
*W*C*CW	21	10	3
*WC*CW	2	1	6
*WC*CW	2	1	6

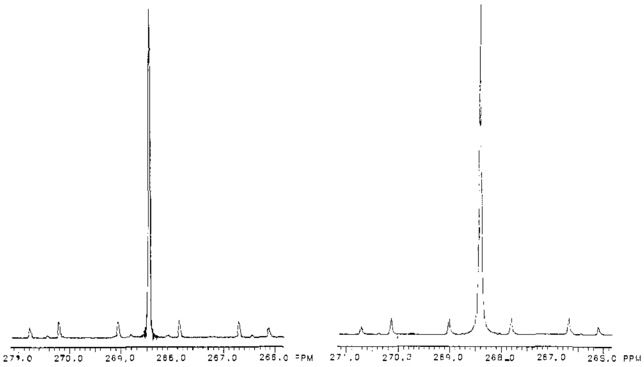

Figure 4. The ^{13}C NMR spectrum due to the alkylidyne carbons of $(t\text{-BuO})_3W\equiv CC\equiv W(O\text{-}t\text{-Bu})_3$ (left) and its spectral simulation (right) in which the alkylidyne carbons are labeled by 92% gatom ^{13}C. The central resonance is skirted by ^{183}W ($I = {}^1/_2$, 14.3% natural abundance) satellites due to three ^{13}C isotopomers: *W*CCW (2% abundance, $^1J(^{183}W-^{13}C) = 300$ Hz), *WC*CW (2% abundance, $^2J(^{183}W-^{13}C) = 55$ Hz), and *W*C*CW (the AA'X pattern, 21% abundance, $^1J(^{13}C-^{13}C) = 44$ Hz).

$(O\text{-}t\text{-Bu})_3\}$ (V), a compound first reported by the Schrock group in 1985.[33] As reported earlier,[33] the complex can be isolated as dark red tablets, and it has a singlet in the ^1H NMR at 1.57 ppm in C_6D_6. We observe a ^{13}C NMR resonance at 268.5 ppm in C_6D_6 which is 10 ppm upfield from the reported value of 278.6 ppm in C_5D_5N.[33] It is known that pyridine coordinates to $(t\text{-BuO})_3W\equiv CMe$ at a position trans to the W≡C bond causing a downfield shift in its ^{13}C NMR resonance.[33] Addition of 6 equiv of pyridine to V in toluene-d_8 does cause a downfield shift in the ^{13}C resonance to 273.7 ppm. Thus, the disparity in the value for the ^{13}C chemical shift in V may be due to varying degrees of pyridine coordination.

Perhaps the best evidence that this product is V is the ^{13}C NMR of V*. Various isotopomers predicted for V* with its 92% g atom ^{13}C label are listed in Table V. Small doublets due to *W*CCW, $^1J(^{183}W-^{13}C) = 300.3$ Hz, and *WC*CW, $^2J(^{183}W-^{13}C) = 54.7$ Hz, are observed as well as an AA'X pattern due to *W*C*CW, $^1J(^{13}C-^{13}C)$. All peaks are in their predicted ratios as shown in Figure 4. A plausible mechanism for formation of V is as shown in eq 2–5 (L = PMe_2Ph).

$$\mathrm{I} + \mathrm{II} \rightarrow trans\text{-}(HC\equiv C)L_2PtC\equiv W(O\text{-}t\text{-Bu})_3 + (t\text{-BuO})_3W\equiv CH \quad (2)$$

$$trans\text{-}(HC\equiv C)L_2PtC\equiv W(O\text{-}t\text{-Bu})_3 + \mathrm{II} \rightarrow trans\text{-}L_2Pt\{C\equiv W(O\text{-}t\text{-Bu})_3\}_2 + (t\text{-BuO})_3W\equiv CH \quad (3)$$

$$trans\text{-}L_2Pt\{C\equiv W(O\text{-}t\text{-Bu})_3\}_2 \rightarrow cis\text{-}L_2Pt\{C\equiv W(O\text{-}t\text{-Bu})_3\}_2 \quad (4)$$

$$cis\text{-}L_2Pt\{C\equiv W(O\text{-}t\text{-Bu})_3\}_2 \rightarrow Pt(L)_n + \mathrm{V} \; (n = 0\text{–}4) \quad (5)$$

$(t\text{-BuO})_3W\equiv CH$ is not detected as a product of the reaction of I with II. This is not surprising since it is thermally unstable over the time scale of the reaction. For example, equilibrium mixtures containing $W_2(O\text{-}t\text{-Bu})_6(\mu\text{-}C_2H_2)py$ and $(t\text{-BuO})_3W\equiv CH$ decompose thermally over a 24-h period,[17] which is comparable to the rate at which V is formed. Even addition of excess PMe_2Ph to solutions of $W_2(O\text{-}t\text{-Bu})_6(\mu\text{-}C_2H_2)py$ does not appear to stabilize $(t\text{-BuO})W\equiv CH$ toward such decomposition. However, the reaction of I with 2 equiv of II *in the presence of 6 equiv of quinuclidine* produces detectable amounts of $(quin)(t\text{-BuO})_3W\equiv CH$ having the reported ^1H NMR resonance at 5.15 ppm ($^2J(^{183}W-^1H) = 90$ Hz).[33] Thus, there is solid evidence for $(t\text{-BuO})_3W\equiv CH$ formation in alkyne metathesis steps such as (2) and (3).

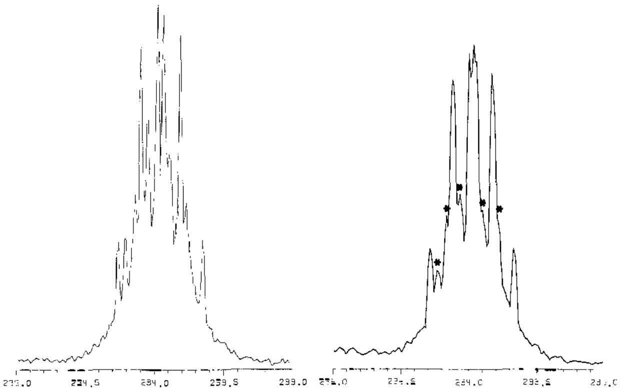

Figure 5. The ^{13}C NMR central multiplet due to the 92% g atom ^{13}C-labeled Pt—*C*═C carbons in *trans*-$Pt[C_2W_2(O\text{-}t\text{-Bu})_5]_2(PMe_2Ph)_2$ (right) where peaks due to the *C═*C—Pt—*C═C isotopomer (17% the intensity of the major isotopomer) are denoted by an asterisk. The left spectrum resulted from the reaction of 2 equiv of $W_2(O\text{-}t\text{-Bu})_6$ with 0.5 equiv of *trans*-$Pt(C\equiv CH)_2(PMe_2Ph)_2$ and 0.5 equiv of its ^{13}C-labeled analogue (see Figure 1). Peaks due to the above-mentioned isotopomer are enhanced in the left spectrum. This is consistent with the reversibility of reaction 2.

Reaction 4, a trans to cis isomerization, and reaction 5, a reductive elimination, have precedence. For example, IV has a trans geometry. However, a less sterically demanding analogue prefers and is able to isomerize to a cis geometry, i.e., *cis*-$Pt\{C_2W_2(O\text{-}i\text{-Pr})_5\}_2(PMe_2Ph)_2$. This cis complex is unstable toward reductive elimination forming $Pt(PMe_2Ph)_4$ and other products (discussed below).

We would expect that the $-C\equiv W(O\text{-}t\text{-Bu})_3$ ligands in *trans*-$L_2Pt\{C\equiv W(O\text{-}t\text{-Bu})_3\}_2$ would have a larger trans influence than either $-C\equiv CH$ or PMe_2Ph and would much rather compete for σ-bonding orbitals with PMe_2Ph than with themselves. Thermodynamically, the cis Pt(II) isomer is therefore favored. Thus, the trans to cis isomerization (4) should occur if it is sterically possible.

When excess PMe_2Ph (4 equiv) is added to a reaction of I and 2 equiv of II, $Pt(PMe_2Ph)_4$ is formed, suggesting that a reductive elimination such as (5) is indeed occurring. $Pt(PMe_2Ph)_4$ formation is not observed in the absence of added phosphine. Apparently, $Pt(PMe_2Ph)_n$ (n = 0–4) undergoes rapid phosphine exchange under these conditions and its ^{31}P NMR peaks are exchange-broadened beyond recognition.

Also there is evidence that reductive elimination steps such as (5) are intramolecular in nature. A reaction was conducted with 0.5 equiv of I, 0.5 equiv of I*, and 2 equiv of II. If (5) is an *intramolecular* reductive elimination, peak ratios for W*C*CW + W*CCW, *W*C*CW, *W*CCW, and *WC*CW in the ^{13}C NMR will remain essentially the same as they are in a reaction with only I* present. If, on the other hand, (5) is *intermolecular*, the relative intensities of peaks for *W*CCW and *WC*CW will be much larger and those for *W*C*CW will be much smaller than in the reaction with only I* present (see Table V). The former case was observed which is consistent with an intramolecular reductive elimination.

The above-described crossover experiment provides evidence that is consistent with the reversibility of reaction 2. The ^{13}C NMR peaks due to the $W_2{}^*C{=}{}^*C{-}Pt{-}{}^*C{=}CW_2$ isotopomer of IV are enhanced in this experiment relative to their size in the reaction with only I* present (see Figure 5). Such an enhancement could be caused by an intermolecular C_2/C_2' or β-carbon scrambling resulting from the reversibility of reaction 2. For example, *trans*-$(H^*C\equiv{}^*C)L_2Pt^*C\equiv W(O\text{-}t\text{-Bu})_3$ could react

---

[33] Listemann, M. L.; Schrock, R. R. *Organometallics* **1985**, *4*, 74.

Table VI. Approximate Time[a] Necessary for the Reactions of Ditungsten Hexaalkoxides with Alkynylplatinum(II) Complexes To Reach 90% Completion at Ambient Temperature

reactns	I + II′	I′ + II′	I + II	I′ + II
time	3–8 min	1.5–2.5 h	4–6 days	no reaction

with $(t\text{-BuO})_3W{\equiv}CH$ to form I-$^{13}C_3$ and II, i.e., reaction −2. I-$^{13}C_3$ could then react with II by way of (1b) eventually forming the above-mentioned $W_2{*}C{=}{*}C{-}Pt{-}{*}C{=}CW_2$ isotopomer of IV-$^{13}C_3$. Less conclusive NMR evidence exists for an enhancement in the $W_2C{=}C{-}Pt{-}C{=}{*}CW_2$ isotopomer of IV. Spectral simulations indicate that a total scrambling of β-carbons does not occur suggesting that the reverse rate of (2) is not significantly faster than its forward rate or the rates of *trans*-$(HC{\equiv}C)L_2Pt{-}C{\equiv}W(O\text{-}t\text{-Bu})_3$ loss.

Reactions of *trans*-$Pt(C{\equiv}CR)_2(PMe_2Ph)_2$ (R = H, Me) with $W_2(O\text{-}i\text{-Pr})_6(py)_2$. The rates for reactions of ditungsten hexaalkoxides with alkynylplatinum(II) complexes are very sensitive to the steric requirements of the accompanying ligands as shown in Table VI. For example, a reaction that takes days, i.e., I + II, is retarded to the point that it is totally unfavorable even at elevated temperatures merely by replacing the acetylenic protons of I by the methyls of *trans*-$Pt(C{\equiv}CMe)_2(PMe_2Ph)_2$ (I′).[18] Because I′ does not react with II, a less bulky dinuclear W(III) compound, $W_2(O\text{-}i\text{-Pr})_6(py)_2$ (II′),[19] was utilized. Here the reaction is complete in a few hours. As a further rate comparison, the reaction of I with II′ occurs in a matter of minutes. The average volume of the cavities between the alkoxide ligands that have the potential for allowing substrates to react with the $W{\equiv}W$ centers is small especially in the case of II. Thus, small changes in the size of the bulky substrates, I or I′, cause a large change in reaction rates.

The reaction of I′ with II′ was investigated because the acid–base chemistry (eq 1b) due to the acidic acetylenic protons in I is eliminated. The observed reaction sequence initiated by $C{\equiv}C$ bond cleavage (eq 1a) parallels that proposed in eq 2–5. The most conclusive evidence for alkyne metathesis is the formation of $W_3(\mu\text{-O-}i\text{-Pr})_3(O\text{-}i\text{-Pr})_6(\mu_3\text{-CMe})$,[12] which is formed from the conproportionation of $(i\text{-PrO})_3W{\equiv}CMe$ and $W_2(O\text{-}i\text{-Pr})_6(py)_2$. $Pt(PMe_2Ph)_4$[34] the ultimate fate of the Pt-containing products of this metathesis, is readily characterized by its ^{31}P NMR signal, δ −34.2 ($^1J(^{195}Pt{-}^{31}P)$ = 3805 Hz). At least one of the major metastable species leading to $Pt(PMe_2Ph)_4$ has a cis geometry.[35] Insufficient data are available at present to propose its exact structure or those of the remaining products since their NMR analysis is complicated by the fluxionality of II′ and various W-containing products. However, alkyne metathesis, trans to cis isomerization about Pt, and reductive elimination appear to be essential features of the total reaction sequence.

The reaction of I with II′ occurs by both (1a) and (1b) with (1a) predominating since $W_2(O\text{-}i\text{-Pr})_6(\mu\text{-}C_2H_2)(py)_2$[14] is a major product. As in the reaction of I′ with II′, the Pt-containing products of metathesis are difficult to characterize by way of ^1H or ^{31}P NMR. Further efforts in their characterization utilizing I* as a reactant were futile since broad, ill-defined ^{13}C NMR resonances between 250 and 285 ppm and between 355 and 365 ppm result as the prime candidates attributable to $Pt{-}C{\equiv}W$ carbons. Whereas $(t\text{-BuO})_3W{\equiv}CR$ are monomeric in solution,[6] the isopropoxide analogues, e.g., $[(HNMe_2)(RC{\equiv})(i\text{-PrO})_2W(\mu\text{-O-}i\text{-Pr})]_2$ (R = Et), can be dimeric both in solution[36] and in the solid state.[9] The ^{13}C NMR resonances for the alkylidyne carbons in these dimers are exchange-broadened due to fluxionality,[36] and it becomes increasingly difficult to reach a slow-exchange limit as the bulk of $RC{\equiv}$ increases. For example, this limit cannot be reached even at −70 °C when R = Et.[35] Thus, it is entirely possible that the $Pt{-}C{\equiv}W(O\text{-}i\text{-Pr})_3$-containing products resulting from the reaction of I with II′ oligomerize and that the fluxionality of the resulting oligomers is the cause for the broad ^{13}C resonances between 250 and 285 ppm. Again, $Pt(PMe_2Ph)_4$ is formed as the ultimate Pt-containing product. As it is formed, the above-described broad resonances are replaced by a mass of sharp singlets in the same general spectral ranges.

Two products of the reaction of I with II′ formed via (1b) lend themselves to a more detailed characterization since they are neither oligomers nor are they fluxional. They have been characterized only as entities of a complex reaction mixture and are unstable toward reductive elimination forming $Pt(PMe_2Ph)_4$.

The initial product *trans*-$Pt(PMe_2Ph)_2(C{\equiv}CH)\{C_2W_2(O\text{-}i\text{-Pr})_5\}$ (VI) has a $PtC_2W_2(OR)_5$ unit which is structurally very similar to that in IV. The ^1H NMR of IV shows two $OCMe_3$ resonances in a 3:2 ratio. That of VI shows two $OCHMe_2$ septets in a 3:2 ratio and three $OCHMe_2$ doublets in a 1:3:1 ratio since the two *i*-PrO groups on W(2) (compare Figure 2) are diastereotopic. The absence of bridging OR groups is noteworthy in IV and VI because, as the oxidation state of similar ditungsten alkoxides increases, a tendency for formation of μ-OR groups becomes evident, e.g., in $W_2(\mu\text{-O-}i\text{-Pr})_2(O\text{-}i\text{-Pr})_4(\mu\text{-}C_2H_2)(py)_2$[14] and $W_2(\mu\text{-O-}t\text{-Bu})_2(O\text{-}t\text{-Bu})_4(\mu\text{-CO})$.[17] Coupling constants and chemical shifts in Table III for VI* are very similar to those observed for III* and IV*.

Complex VI is intermediate in the formation of *cis*-$Pt(PMe_2Ph)_2\{C_2W_2(O\text{-}i\text{-Pr})_5\}_2$ (VII). The diversity and complexity of product spectra present in the ^1H NMR when the concentration of the intermediate VII is maximum makes unequivocal assignment of its (O-*i*-Pr) NMR resonances almost impossible. However, several lines of evidence are in harmony with a cis geometry. In the ^1H NMR, PMe_2Ph resonances indicative of a cis geometry about platinum[35] parallel the rise and fall of ^{31}P and ^{13}C resonances attributed to VII*. In the ^{31}P and ^{13}C NMR of VII*, an AA′MM′XX′ or $C_1C_1'C_2C_2'PP'$ pattern should be observed. The ^{13}C NMR spectrum was simulated readily by such a coupling pattern although a satisfactory simulation of the ^{31}P NMR was never achieved. A doublet coupling of 40.4 Hz assigned to $\{^2J(^{31}P{-}^{13}C) + {}^2J(^{31}P{-}^{13}C')\}$ is evident in both spectra and is further evidence for the cis geometry about Pt.

Although the chemical shifts for VII and VII* in Table III parallel those observed for the trans derivatives III, IV, and VI, the coupling constants to ^{195}Pt are considerably larger suggesting that both Pt–P and Pt–C bonding are stronger in the former. Obviously, the cis geometry in VII is thermodynamically more stable than the trans. This implies that the structurally related IV is kinetically stabilized toward the otherwise thermodynamically favored trans to cis isomerization by the steric bulk of its $C_2W_2(O\text{-}t\text{-Bu})_5$ ligands. This is also why IV is thermally stable to 75 °C: the cis geometry necessary for reductive elimination is sterically inaccessible. On the other hand, complexes containing smaller $-C{\equiv}W(OR)_3$ and/or $-C_2W_2(OR)_5$ entities are kinetically labile forming a host of uncharacterized mono- or oligomeric products via sterically allowed trans to cis isomerizations.

Reactivity of IV. Although H_2O and O_2 sensitive, this complex is thermally stable to at least 75 °C. Efforts have been initiated to probe the reactivity of the $PtP_2(C_2W_2O_5)_2$ core of this molecule. Since the C_2 unit is potentially nucleophilic, reactions with Lewis acids will be attempted. The reaction of IV with BCl_3 yielded a dark, insoluble precipitate and $BCl_n(O\text{-}t\text{-Bu})_{3-n}$ in the supernatant liquid. Iodine and related oxidizing reagents could either oxidize Pt(II) or add to the C(4)–C(5) multiple bond or the W(2)–W(3) multiple bond. The reaction of I_2 with IV produces a reddish brown precipitate that is totally insoluble in common organic solvents. The exact composition of this solid has not been investigated further. PMe_2Ph lability in IV and its reaction with CO will now be discussed.

Rates of PMe_2Ph Exchange. Rates of PMe_2Ph exchange in I, III, and IV are retarded as the steric bulk of the ligands around Pt increases; i.e., PMe_2Ph exchange follows the order I > III ≫

---

(34) Mann, B. E.; Musco, A. *J. Chem. Soc., Dalton Trans.* **1980**, 776.

(35) Resonances for PMe_2Ph and the ortho protons in PMe_2Ph are split into triplets due to virtual coupling in trans-Pt complexes, but only into doublets in cis-Pt complexes. For the proposed cis complex resulting from the reaction of I′ with II′: $\delta(PMe_2Ph)$ 2.23 (d, $^2J(^{31}P{-}^1H)$ = 10.8 Hz, $^3J(^{195}Pt{-}^1H)$ = 33 Hz), $\delta(PMe_2Ph$, ortho-H) 7.87 (dd, $^3J(^{31}P{-}^1H)$ = 12 Hz, $^3J(^1H{-}^1H)$ = 8.2 Hz, $^nJ(^1H\text{-unassigned})$ = 1.8 Hz). For VI: $\delta(PMe_2Ph)$ 2.23 (d, $^2J(^{31}P{-}^1H)$ = 10.5 Hz, $^3J(^{195}Pt{-}^1H)$ = 35 Hz), $\delta(PMe_2Ph$, ortho H) 7.9 (dd).

(36) Chisholm, M. H.; Conroy, B. K., unpublished results.

Table VII. The $^1J(^{195}Pt-^{31}P)$ Values (Hz) and ^{31}P NMR Chemical Shifts (ppm) for Pt(II) Complexes Containing $-C_2W_2(OR)_5$ or $-C_2W_2(\mu\text{-}CO)(OR)_5$ Ligands

complex	I	III	IV	VIII	IX	VI	VII
$^1J(^{195}Pt-^{31}P)$	2447	2591	2776	2714	2672	2757	3171
$\delta(PMe_2Ph)$	−14.7	−11.2	−8.0	−8.4	−9.2	−7.6	−3.7

IV. NMR data supporting these relative rates can be derived from (a) Pt—C≡C*H* resonances, (b) ortho-H resonances of PMe_2*Ph*, and (c) *P*Me_2Ph resonances. (i) The NMR spectra of solutions containing pure I show virtual coupling of the two ^{31}P nuclei in I to Pt—C≡C*H*. After 18 h of the reaction of I with II, this ^{31}P coupling in I is not observed due to rapid phosphine exchange whereas the triplet nature of the Pt—C≡C*H* resonance in III is evident. Therefore, phosphine exchange in I is more rapid than in III. In a similar reaction solution containing 4 equiv of PMe_2Ph, the resonance in III has also reached the fast-exchange limit. (ii) Without PMe_2Ph added, three separate ortho-H resonances can be observed in the ^1H NMR for solutions containing I, III, and IV. When 4 equiv of PMe_2Ph are present, a separate resonance for IV and an exchange-averaged signal for PMe_2Ph, I, and III are observed. Thus, phosphine exchange in IV is much slower than in I and III. (iii) Solutions containing I, III, and IV exhibit sharp ^{31}P NMR signals for III and IV, but the I resonance is exchange-broadened. When 4 equiv of PMe_2Ph are present, a sharp peak is observed again for IV, but the I, III, and PMe_2Ph resonances are exchange-averaged and centered at −39.5 ppm after 18 h, −43.4 ppm after 44 h, and −45.3 ppm after 90 h. The resonance for free PMe_2Ph is at −45.7 ppm. The above data suggest that the Pt atom in IV is substitutionally inert. Ligand substitution in square-planar complexes is associative in nature in noncoordinating solvents and occurs via a five-coordinate intermediate. Formation of such an intermediate from IV is highly disfavored due to the steric bulk of the two $-C_2W_2(O\text{-}t\text{-}Bu)_5$ ligands. This may also suggest that other bimolecular, Pt-centered reactions of IV will also be sluggish at best (e.g., oxidative additions).

Reaction of IV with CO. The addition of 1 or 2 equiv of CO to IV forms two closely related complexes in a sequential manner. When ^{13}CO is utilized, ^{13}C NMR resonances for the initial product, $\delta(CO)$ 303.3 ($^1J(^{183}W-^{13}C)$ = 148 Hz), and final product, $\delta(CO)$ 303.1 ($^1J(^{183}W-^{13}C)$ = 150 Hz), are readily observed. These chemical shifts and coupling constants are analogous to those found for $W_2(\mu\text{-}CO)$ resonances of $W_2(OCH_2CMe_3)_6(py)_2(\mu\text{-}CO)$ and related complexes.[17] Apparently CO adds to the W=W bonds of IV forming *trans*-$Pt(PMe_2Ph)_2\{C_2W_2(O\text{-}t\text{-}Bu)_5\}\{C_2W_2(\mu\text{-}CO)(O\text{-}t\text{-}Bu)_5\}$ (VIII) and *trans*-$Pt(PMe_2Ph)_2\{C_2W_2(\mu\text{-}CO)(O\text{-}t\text{-}Bu)_5\}_2$ (IX) in successive steps. The doublet of triplets nature of the PMe_2*Ph* ortho-hydrogen resonances is indicative of the trans geometry.

The $^1J(^{195}Pt-^{31}P)$ resonances of VIII, IX, and other related complexes readily show the relative cis influence[37] of the −C≡CH, $-C_2W_2(OR)_5$, and $-C_2W_2(\mu\text{-}CO)(O\text{-}t\text{-}Bu)_5$ ligands. See Table VII. The -C≡CH ligand, which is isoelectronic with −CO, is a π-acceptor, and π-donation from Pt-centered orbitals such as d_{xy} tends to weaken the C≡C bond; e.g., ν(C≡C) in I is 1959 cm^{-1} vs. 2140–2100 cm^{-1} in RC≡CH. The PMe_2Ph ligands in I can also act as π-acceptors and compete with cis-oriented ligands for Pt d_{xy} orbital electron density. In the sequence I–III–IV, $^1J(^{195}Pt-^{31}P)$ values increase signaling increasingly stronger Pt–P bonds.[37] The $-C_2W_2(O\text{-}t\text{-}Bu)_5$ ligand does not compete as readily with PMe_2Ph for Pt π-electrons as does the −C≡CH ligand: The W_2 center is pumping electron density into the π*-orbitals of the C_2 unit; thus it has a lower capacity to accept π-electron density from Pt. Since $^1J(^{195}Pt-^{31}P)$ decreases in the series IV–VIII–IX, the $-C_2W_2(\mu\text{-}CO)(O\text{-}t\text{-}Bu)_5$ ligand must have a larger cis influence than $-C_2W_2(O\text{-}t\text{-}Bu)_5$. This is reasonable: μ-CO is now competing with the C_2 unit for π-electron density on the W_2 center. Therefore, the C_2 unit has a greater capacity to accept π-electron density from Pt. The $-C_2W_2(O\text{-}i\text{-}Pr)_5$ ligand has a smaller cis influence than the bulkier $-C_2W_2(O\text{-}t\text{-}Bu)_5$ since the $^1J(^{195}Pt-^{31}P)$ in VI is larger than that in the isostructural III. The smaller O-*i*-Pr ligands in the former allow stronger W_2–C_2 bonding. The C_2 unit, in turn, has a smaller capacity to accept π-electron density from Pt. From the above data, a cis influence scale can be created: −C≡CH > $-C_2W_2(\mu\text{-}CO)(O\text{-}t\text{-}Bu)_5$ > $-C_2W_2(O\text{-}t\text{-}Bu)_5$ > $-C_2W_2(O\text{-}i\text{-}Pr)_5$. It is unfortunate that insufficient data are present to add the $-C{\equiv}W(OR)_3$ moiety to this series. The consistent upfield shift in $\delta(^{31}P)$ with increasing $^1J(^{195}Pt-^{31}P)$ should also be noted.

Projected Synthesis and Characterization of Acetylide and Carbide Clusters Supported by Alkoxides. The above results have opened new vistas for research. For example, acetylide complexes, $(R'C{\equiv}C)W_2(OR)_5$, similar in structure to a $(PtC{\equiv}C)W_2(OR)_5$ unit in IV could possibly be synthesized by the reaction of $LiC{\equiv}CR'$ with $W_2(OR)_6L_n$ yielding LiOR as a byproduct. The reaction could possibly proceed a step further for LiC≡CH yielding an alkoxide-supported dicarbido cluster of tungsten, LiOR, and ROH.

Another potential route to carbido clusters may result from the use of Pt or Pd complexes such as I as templates for the formation small carbido clusters that might form larger clusters after reductive elimination has been induced. For example, conditions could possibly be optimized to form $W_4C_4(OR)_{10}$ clusters from the controlled alcoholysis of IV by ROH where R = isopropyl, neopentyl, ethyl, etc. Similar reactions could be attempted for IX.

Characterization of larger clusters becomes increasingly difficult. Introduction of a ^{13}C label into these clusters by way of H*C≡*CH would not be too arduous of a task. Another tool that may prove useful in their characterization is ^{183}W NMR.[38] This would be especially useful when crystals suitable for X-ray crystallography were not available.

The ^{183}W NMR of IV. The ^{183}W NMR spectrum of IV shown in Figure 6 reveals two resonances where δ(W(2)) 4733 ($^2J(^{195}Pt-^{183}W)$ = ~41 Hz) and δ(W(1)) 4567. These resonances are very close to that of the parent $W_2(O\text{-}t\text{-}Bu)_6$, δ 4408,[39] when the total chemical shift range for ^{183}W NMR of 11 000 ppm[38] is considered. Each ^{183}W resonance is skirted by ^{183}W satellites with $^1J(^{183}W-^{183}W)$ = 252 Hz. The two sets of satellites are an AB quartet (b/a = 0.82); i.e., each central resonance is at the center of mass and not the actual center of its pair of satellites. The former centers are displaced 6 Hz from the latter toward the center of the AB quartet. This, to our knowledge, is the first reported example of a *one bond* W–W coupling constant. Several *two-bond* W–O–W coupling constants have been reported.[38] Work is in progress to obtain further $^1J(^{183}W-^{183}W)$ as a function of W–W bond order.

Experimental Section

Reagents and General Techniques. General procedures and the preparations of $W_2(O\text{-}i\text{-}Pr)_6(py)_2$ and $W_2(O\text{-}t\text{-}Bu)_6$ have been described.[19] Quinuclidine was purchased from Lancaster Synthesis Ltd. and was used without further purification. Ethyne and carbon monoxide were purchased from Matheson and were used without further purification. Dry and oxygen-free hexane, toluene, tetrahydrofuran, and pyridine were used in all preparations. The elemental analysis was performed by Alfred Bernhardt Microanalytisches Laboratorium, West Germany.

NMR samples were prepared by using dry and oxygen-free toluene-d_8 or benzene-d_6. ^1H and ^{13}C NMR spectra were recorded on a Varian XL-300 instrument at 300 and 75.45 MHz, respectively. All ^1H NMR chemical shifts are in parts per million relative to either the C_6D_5H singlet of C_6D_6 set at δ 7.15 or the CHD_2 quintet of toluene-d_8 set at δ 2.09. ^{13}C NMR chemical shifts are in parts per million relative to the C_6D_6 triplet at δ 128.0 or the C_α heptet of toluene-d_6 at 20.4 ppm. The ^{13}C NMR spectra were obtained for products derived from reactions using either the labeled *trans*-$Pt(PMe_2Ph)_2(1,2\text{-}^{13}C_2\text{-}C{\equiv}CH)_2$ or ^{13}C-CO. The ^{13}C-labeled ethyne used in the synthesis of the former and the ^{13}C-labeled CO were purchased from MSD isotopes and used without

---

[37] Blau, Reed J.; Espenson, J. H. *Inorg. Chem.* **1986**, *25*, 878 and references therein.

[38] Minelli, M.; Enemark, J. H.; Brownlee, R. T.; O'Connor, M. J.; Wedd, A. G. *Coord. Chem. Rev.* **1985**, *68*, 169.

[39] Young, C. S.; Enemark, J. H.; Kober, E. *Polyhedron* **1987**, *6*, 255.

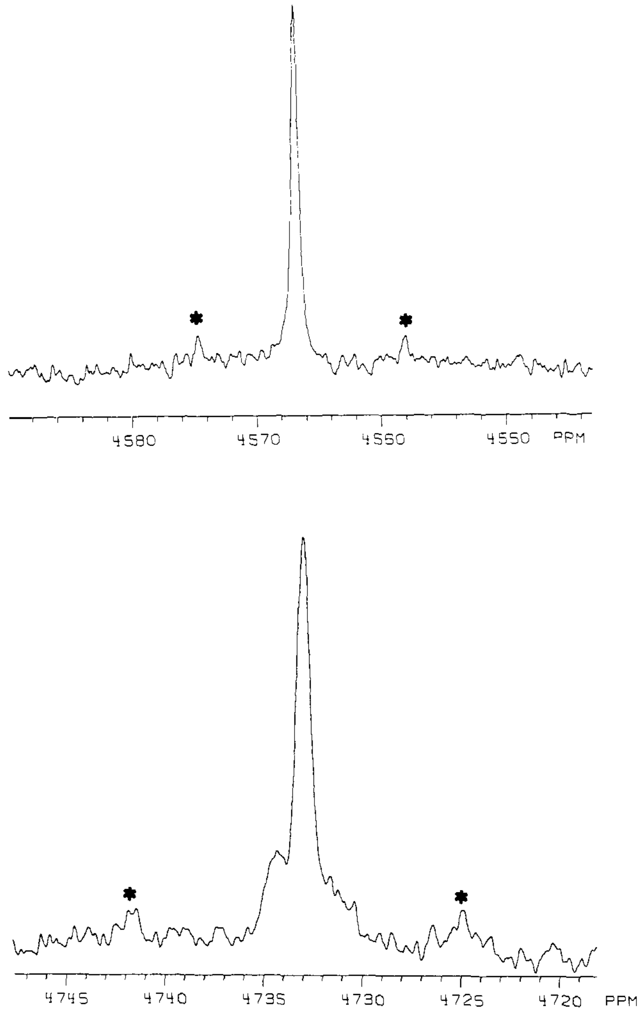

Figure 6. The ^{183}W NMR signals for *trans*-Pt[C_2W_2(O-*t*-Bu)$_5$]-(PMe_2Ph)$_2$. One resonance is flanked by distorted ^{195}Pt satellites (^2J-(^{195}Pt–^{183}W(2)) $\simeq$ 41 Hz) (bottom) and is assigned to W(2) in Figure 1. Each resonance is accompanied by a set of ^{183}W satellites indicated by an asterisk that are barely visible above the noise level. The two pairs of ^{183}W satellites are an AB quartet where ^1J(^{183}W(1)–^{183}W(2)) = 252 Hz.

further purification. ^{31}P NMR spectra were recorded on a Varian XL-100 at 40.5 MHz. ^{31}P chemical shifts are reported relative to 85% H_3PO_4.

Infrared spectra were recorded on a Perkin-Elmer 283 spectrophotometer as Nujol or Fluorolube mulls between NaCl plates.

^{13}C NMR Simulations. ^{13}C NMR simulations were conducted on a Nicolet NT-360 360-MHz spectrometer using the accompanying NMCSIM software. Coupling patterns for the major isotopomers (>5% abundance) of I*, III*, and IV* were calculated separately and added individually to a composite spectrum as the appropriate fraction of the total spectrum. Comparisons between experimental and calculated spectra were visual in nature.

^{183}W NMR of IV. A 0.9-g sample of IV and 2.5 mL of C_6D_6 were sealed in a 10-mm NMR tube. The solid was not totally dissolved at ambient temperature; thus spectra were taken at 35 °C yielding a solution ~0.2 M in IV. Chemical shifts are in parts per million relative to Na_2WO_4. Spectra were taken on a Nicolet NT 360-MHz spectrometer at 15.11 MHz. Initial spectra were taken with a very large window, ±10 000 Hz. Additional spectra were accumulated with a smaller window to improve resolution and to verify that the resonances were not "folded over". Preliminary spectra were accumulated overnight. The final spectrum was accumulated for ~64 h with 28 810 scans. The pulse width was 40 μs followed by a 5-s delay. The sweep width was ±2500 Hz with the spectrometer frequency at 15.112 877 MHz and an offset of 69 732 Hz from Na_2WO_4.

***trans*-Pt(PMe_2Ph)$_2$(C≡CH)$_2$.** This complex was synthesized from the reaction of *cis*-$PtCl_2$(PMe_2Ph)$_2$ and LiC≡CH according to the literature[18] with the exception that a 30% rather than a 60–100% excess of *n*-butyllithium is utilized in the in situ formation of LiC≡CH from ethyne.

The $^{13}C_4$-labeled complex was synthesized similarly by using 230 mg of *cis*-$PtCl_2$(PMe_2Ph)$_2$, a 30% excess of *n*-butyllithium, and only a 50% excess ^{13}C-labeled ethyne. The reaction yielded ~140 mg of pure product.

NMR data are for I and I* in C_6D_6. ^{1}H NMR: δ(≡CH) 2.38 (t, 2 H, ^3J(^{195}Pt–^{1}H) = 45 Hz, ^4J(^{31}P–^{1}H) = 2.3 Hz); δ(PMe) 1.81 (t, 12 H, ^3J(^{195}Pt–^{1}H) = 33 Hz, ^2J + ^4J(^{31}P–^{1}H) = 7.8 Hz), δ(PPh–ortho H) 7.82 (dt, 4 H, ^3J(^{1}H–^{1}H) = 6 Hz, ^3J(^{31}P–^{1}H) = 6.0 Hz). ^{31}P NMR: δ-(PMe_2Ph) −14.7 (s, ^1J(^{195}Pt–^{31}P) = 2447 Hz). ^{13}C NMR for $HC_\beta \equiv C_\alpha - Pt - C_\alpha' \equiv C_\beta'H$: $\delta(C_\alpha)$ 100.7 (t, ^1J(^{195}Pt–$^{13}C_\alpha$) = 948 Hz, ^2J-($^{13}C_\alpha$–^{1}H) = 42 Hz, ^2J(^{31}P–$^{13}C_\alpha$) = 15.0 Hz); $\delta(C_\beta)$ 94.9 (s, ^2J(^{195}Pt–$^{13}C_\beta$) = 266 Hz, ^1J($^{13}C_\beta$–^{1}H) = 224 Hz). ^{13}C NMR for I*: ^1J-($^{13}C_\alpha$–$^{13}C_\beta$) = 122 Hz, ^3J($^{13}C_\alpha$–$^{13}C_\beta'$) = 10.5 Hz, ^2J($^{13}C_\alpha$–$^{13}C_\alpha'$) = 40 Hz).

***trans*-Pt(PMe_2Ph)$_2$(C≡CH){C_2W_2(O-*t*-Bu)$_5$}.** The reaction of a 1:1 stoichiometry of I with II in toluene yields ultimately a mixture containing I, III, IV, and V. After the solvent was stripped, unreacted I can be separated from the products by extraction of the products into hexanes leaving the insoluble I as a residue. Although III is less soluble than IV or V in hexanes, it was never isolated as a pure crystalline solid.

NMR data are for III and III* in C_6D_6. ^{1}H NMR: δ(≡C*H*) 2.40 (t, 1 H, ^3J(^{195}Pt–^{1}H) = 43 Hz, ^2J + ^4J(^{31}P–^{1}H) = 4.3 Hz); δ(PMe) 1.79 (t, 12 H, ^3J(^{195}Pt–^{1}H) = 32 Hz, ^2J + ^4J(^{31}P–^{1}H) = 7.2 Hz); δ(O-*t*-Bu) 1.56 (s, 36 H); δ(O-*t*-Bu′) 1.53 (s, 54 H); δ(PPh–ortho H) 7.9 (dt, H, ^3J(^{1}H–^{1}H) = 6.4 Hz, ^3J(^{31}P–^{1}H) = 5 Hz). ^{31}P NMR: δ(PMe_2Ph) −11.2 (s, ^1J(^{195}Pt–^{31}P) = 2591 Hz). ^{13}C NMR for $HC_\beta \equiv C_\alpha$-Pt-$C_1 = C_2$: $\delta(C_\alpha)$ 100.5 (t, ^1J(^{195}Pt–$^{13}C_\alpha$) = 941 Hz, ^2J(^{31}P–$^{13}C_\alpha$) = 16.0 Hz) $\delta(C_\beta)$ 97.12 (s, ^2J(^{195}Pt–$^{13}C_\beta$) = 259 Hz); $\delta(C_1)$ 235.2 (t, ^1J(^{195}Pt–$^{13}C_1$) = 802 Hz; ^2J(^{31}P–$^{13}C_1$) = 11.5 Hz); $\delta(C_2)$ 302.1 (t, ^2J(^{195}Pt–$^{13}C_2$) = 78.2 Hz, ^1J-(^{183}W(1)–$^{13}C_2$) = 132 Hz, ^3J(^{31}P–$^{13}C_2$) = 2 Hz). ^{13}C NMR of III*: ^1J($^{13}C_\alpha$–$^{13}C_\beta$) = 122.2 Hz, ^2J($^{13}C_\alpha$–$^{13}C_1$) = 36.2 Hz, ^3J($^{13}C_\alpha$–$^{13}C_2$) = 3.3 Hz, ^1J($^{13}C_1$–$^{13}C_2$) = 18.5 Hz, ^3J($^{13}C_1$–$^{13}C_\beta$) = 12.0 Hz.

***trans*-Pt(PMe_2Ph)$_2${C_2W_2(O-*t*-Bu)$_5$}$_2$.** W_2(O-*t*-Bu)$_6$ (1.0 g, 1.24 mmol) and *trans*-Pt(PMe_2Ph)$_2$(C≡CH)$_2$ (0.32 g, 0.62 mmol) were added to a 30-mL Schlenk reaction vessel followed by 10 mL of toluene. The burgundy solution turns slowly to a golden brown. After 5 days of reaction at 30 °C, the toluene volume was reduced 50% and the resulting solution was cooled to −15 °C overnight. This procedure yielded 0.58 g of crystalline IV (brown crystals) contaminated with ~10% of amorphous V. A further recrystallization in hexanes of solids from the supernatant liquid yielded an additional 0.32 g of solid with comparable purity. IV may be depleted of V by a careful crystallization of V from solutions of IV and V in toluene by slowly cooling. The elemental analysis is reported in Table IV.

NMR data are for IV and IV* in C_6D_6. ^{1}H NMR: δ(PMe) 1.77 (t, 12 H, ^3J(^{195}Pt–^{1}H) = 30 Hz, ^2J + ^4J(^{31}P–^{1}H) = 6.9 Hz); δ(O-*t*-Bu) 1.51 (s, 36 H); δ(O-*t*-Bu) 1.48 (s, 54 H); δ(PPh–ortho H) 8.0 (dt, 4 H, ^3J(^{1}H–^{1}H) = 7 Hz, ^3J(^{31}P–^{1}H) = 6 Hz). ^{31}P NMR: δ(PMe_2Ph) −8.0 (s, ^1J(^{195}Pt–^{31}P) 2776 Hz). ^{13}C NMR for $C_2' = C_1'$-Pt-$C_1 = C_2$: $\delta(C_1)$ 233.9 (t, ^1J(^{195}Pt–$^{13}C_1$) = 801 Hz, ^1J(^{183}W(2)–$^{13}C_1$) = 50.5 Hz, ^2J(^{31}P–$^{13}C_1$) = 12.5 Hz); $\delta(C_2)$ 302.1 (t, ^1J(^{183}W(1)–$^{13}C_2$) = 133 Hz, ^2J-(^{195}Pt–$^{13}C_2$) = 76.3 Hz, ^3J(^{31}P–$^{13}C_2$) = 2.2 Hz). ^{13}C NMR for IV*: AA′LL′XX′ pattern where N = ^1J + ^3J($^{13}C_1$–$^{13}C_2$) = 21.6 Hz. Reasonable simulation of the central resonances may be obtained for ^1J-($^{13}C_1$–$^{13}C_2$) = 18.5 Hz, ^3J($^{13}C_1$–$^{13}C_2'$) = 3.1 Hz, ^2J($^{13}C_1$–$^{13}C_1'$) = 39.4 Hz. ^{195}Pt{^{1}H} NMR: δ(Pt) −4565 (t). ^{183}W NMR: δ W(1) 4567 (s, ^1J(^{183}W(1)–^{183}W(2)) = 252 Hz); δ W(2) 4733 (s, ^2J(^{195}Pt–^{183}W(2)) = 41 Hz).

IR (cm^{-1}): in Nujol, 1255 w, 1230 m, 1170 s, 1100 w, 1020 m, 995 m, 957 s, 947 s, 930 m, 842 w, 790 m, 737 m, 720 w, 480 w; in Fluorolube, 2982 s, 2910 m, 1383 m, 1358 s.

[(*t*-BuO)$_3$W≡C]$_2$. This complex is a minor product in the synthesis of IV described above. It can be isolated from the reaction mixture in toluene by slowly cooling the solution. Pure reddish brown tablets can be isolated.

NMR data are for V and V* in C_6D_6. ^{1}H NMR: δ(O-*t*-Bu) 1.57 (s). ^{13}C NMR of V*: δ(W≡C) 268.5 (s, ^1J(^{183}W–^{13}C) = 300.3 Hz, ^2J-(^{183}W–^{13}C) = 54.7, ^1J(^{13}C–^{13}C′) = 44.5 Hz).

Reactions in Sealed NMR Tubes. Reactions were often followed in sealed NMR tubes especially in earlier stages of product characterization and in reactions involving ^{13}C-labeled materials. In the case of very complicated reactions, e.g., I′ + II′ and I + II′, serious attempts at product isolation have not been made, and the products have only been characterized as entities of a complex reaction mixture by NMR techniques.

Typically, 60–120 mg (0.070–0.150 mmol) of [W(III)]$_2$ were added to 20–40 mg (0.035–0.070 mmol) of Pt(II) in a 5-mm NMR tube with a 4 in. long, 5 mm (outer diameter), Pyrex glass extension. Approximately 0.6 mL of deuteriated solvent was added, the solution was frozen to −196 °C, and the NMR tube was evacuated and sealed. Facile re-

Table VIII. Summary of Crystallographic Data for IV

fw	1985.98
space group	$P\bar{1}$
a, Å	11.983 (5)
b, Å	17.413 (9)
c, Å	10.574 (4)
α, deg	92.31 (2)
β, deg	107.87 (2)
γ, deg	108.59 (2)
Z	1
V, Å^3	1966.89
d_{calcd}, g/cm^{-1}	1.677
linear abs coeff, cm^{-1}	78.269
temp, °C	−155
sample to source dist, cm	23.5
takeoff angle, deg	2.0
scan width, deg	$1.8 + 0.692 \tan\theta$
2θ range, deg	6–45
data collected	6696 total
unique data with $F_o > 2.33\sigma(F_o)$	4544
cryst size, mm	0.10 × 0.10 × 0.10
cryst color	reddish brown
radiatn	Mo K$\bar{\alpha}$ (λ = 0.71069 A), graphite monochromator
instrument	Picker four-circle diffractometer locally modified and interfaced
detector aperture	3.0 mm wide × 4.0 mm high, 22.5 cm from crystal
scan speed, deg/min	4.0
bkgd counts, s, at each end of scan	10
unique data	5162
$R(F)$	0.0353
$R_w(F)$	0.0360
goodness of fit	0.914
largest Δ/σ	0.05

actions were followed by using low temperature NMR techniques. NMR data for new complexes characterized in this manner without isolation are presented below.

***trans*-Pt(PMe$_2$Ph)$_2$(C≡CH){C$_2$W$_2$(O-*i*-Pr)$_5$}.** This product is formed from the reaction of *trans*-Pt(PMe$_2$Ph)$_2$(C≡CH)$_2$ with W$_2$(O-*i*-Pr)$_6$(py)$_2$ at temperatures above 5 °C. In the presence of excess II′, it rapidly ($t_{1/2} \simeq$ 20 min) undergoes further reaction(s) at ambient temperature.

NMR data are for VI and VI* in toluene-d_8. ^{1}H NMR: δ(PPh–ortho H) 7.82 (dt, 4 H); δ(OC*H*Me$_2$) 5.27 (septet, 2 H, $^3J(^1\mathrm{H}{-}^1\mathrm{H})$ = 6 Hz), 4.87 (septet, 3 H, $^3J(^1\mathrm{H}{-}^1\mathrm{H})$ = 6 Hz); δ(OCH*Me*$_2$) 1.48 (d, 6 H), 1.32 (d, 18 H), 1.19 (d, 6 H). ^{31}P NMR: δ(PMe$_2$Ph) −7.6 (s, $^1J(^{195}\mathrm{Pt}{-}^{31}\mathrm{P})$ = 2757). ^{13}C NMR for VI*; $\mathrm{HC_\beta{\equiv}C_\alpha{-}Pt{-}C_1{=}C_2}$: $\delta(\mathrm{C_1})$ 227.8 ($^1J(^{195}\mathrm{Pt}{-}^{13}\mathrm{C}_1)$ = 814 Hz); $\delta(\mathrm{C_2})$ 284.3 ($^2J(^{195}\mathrm{Pt}{-}^{13}\mathrm{C}_2)$ = 86 Hz); $\delta(\mathrm{C}_\alpha$ and $\mathrm{C}_\beta)$ 94–100 ($^1J(^{13}\mathrm{C}_\alpha{-}^{13}\mathrm{C}_\beta)$ = 122 Hz).

***cis*-Pt(PMe$_2$Ph)$_2${C$_2$W$_2$(O-*i*-Pr)$_5$}$_2$.** This product is formed from the reaction of I with 2II′ where $t_{1/2} \simeq$ 20 min at ambient temperature. It decomposes thermally in solution in a matter of hours.

NMR data are for VII and VII* in toluene-d_8. ^{1}H NMR: δ(PPh–ortho H) 7.9 (dd, 4 H, $^3J(^{31}\mathrm{P}{-}^1\mathrm{H})$ = 11.7 Hz, $^3J(^1\mathrm{H}{-}^1\mathrm{H})$ = 6.9 Hz); δ(PMe) 2.23 (d, 12 H, $^3J(^{195}\mathrm{Pt}{-}^1\mathrm{H})$ = 35 Hz). ^{31}P NMR: δ(PMe$_2$Ph) −3.7 (s, $^1J(^{195}\mathrm{Pt}{-}^{31}\mathrm{P})$ = 3171. ^{13}C NMR for VII* ($\mathrm{Pt{-}C_1{=}C_2}$): $\delta(\mathrm{C_1})$ 216.9 ($^1J(^{195}\mathrm{Pt}{-}^{13}\mathrm{C})$ = 983 Hz, $\{^2J(^{31}\mathrm{P}{-}\mathrm{C}_1) + {}^2J(^{31}\mathrm{P}{-}\mathrm{C}_2')\}$ = 40.4 Hz); $\delta(\mathrm{C_2})$ 282.3 ($^2J(^{195}\mathrm{Pt}{-}^{13}\mathrm{C})$ = 115 Hz, $^1J(\mathrm{C}_1{-}\mathrm{C}_2)$ = 19 Hz). Reasonable simulation of C$_1$ and C$_2$ may be obtained by using $^2J(^{13}\mathrm{C}_1{-}^{13}\mathrm{C}_1')$ = 7.4 Hz, $^2J(^{31}\mathrm{P}{-}^{31}\mathrm{P})$ = 16.6 Hz, $^2J(^{31}\mathrm{P}{-}^{13}\mathrm{C}_1)$ = 25.8 Hz, $^2J(^{31}\mathrm{P}{-}^{13}\mathrm{C}_2)$ = 15.5 Hz. Although simulation of the ^{31}P multiplet (ddd) of VII* was unsatisfactory, couplings of 40, 17, and 7 Hz appear to be present.

Reactions of CO with IV in NMR Tubes. The analysis of reactions of CO with IV are only at a preliminary stage at present. Typically, ~0.6 mL of toluene-d_8 was added to 50–80 mg (0.025–0.04 mmol) of IV in an NMR tube. A septum was secured on the top of the tube, the sample was cooled to −78 °C, and the proper amount of CO or ^{13}C-labeled CO was injected into the tube via a gas-tight syringe. After CO addition, the septum and top of the tube were wrapped with parafilm and the tube was shaken vigorously. The solution was kept near −78 °C until it was analyzed by ambient- or low-temperature NMR. NMR data for products characterized in this fashion follow.

***trans*-Pt(PMe$_2$Ph)$_2${C$_2$W$_2$(O-*t*-Bu)$_5$}{C$_2$W$_2$(μ-CO)(O-*t*-Bu)$_5$} (VIII).** This complex is formed from the reaction of 1 equiv of CO with IV at temperatures above 0 °C. In the absence of excess CO, this product appears to be thermally stable at ambient temperature.

NMR data are for VIII in toluene-d_8. ^{1}H NMR: δ(PPh-ortho H) 8.13 (dt, 4 H, $^3J(^1\mathrm{H}{-}^1\mathrm{H})$ = 6.8 Hz, $^3J(^{31}\mathrm{P}{-}^1\mathrm{H})$ = 6 Hz); δ(O-*t*-Bu) 1.503 (s, 18 H); δ(O-*t*-Bu) 1.426 (s, 27 H); *t*-BuO ligands on the −C$_2$W$_2$(μ-CO)(O-*t*-Bu)$_5$ unit appear to be fluxional at room temperature. ^{31}P NMR: δ(PMe$_2$Ph) −8.4 ($^1J(^{195}\mathrm{Pt}{-}^{31}\mathrm{P})$ = 2714 Hz). ^{13}C NMR: δ(μ-CO) 303.3 ($^1J(^{183}\mathrm{W}{-}^{13}\mathrm{C})$ = 148 Hz).

***trans*-Pt(PMe$_2$Ph)$_2${C$_2$W$_2$(μ-CO)(O-*t*-Bu)$_5$}$_2$ (IX).** This complex is formed from the reaction of 2 equiv of CO with IV at temperatures above 10 °C. Reaction of IV with more than 2 equiv of CO forms W(CO)$_6$ and other uncharacterized products.

NMR data are for IX in toluene-d_8. ^{1}H NMR: δ(PPh-ortho H) 8.36 (dt, 4 H, $^3J(^1\mathrm{H}{-}^1\mathrm{H})$ = 6.5, $^3J(^{31}\mathrm{P}{-}^1\mathrm{H})$ = 6.6 Hz); δ(PMe) 1.135 (t, 12 H); *t*-BuO ligands appear to be fluxional at ambient temperature. ^{31}P NMR: δ(PMe$_2$Ph) −9.2 ($^1J(^{195}\mathrm{Pt}{-}^{31}\mathrm{P})$ = 2672 Hz). ^{13}C NMR: δ(μ-CO) 303.1 ($^1J(^{183}\mathrm{W}{-}^{13}\mathrm{C})$ = 150 Hz).

Crystallographic Study of IV. General operating facilities and listings of programs have been given previously.[40] Crystal data for IV are found in Table VIII.

A suitable small crystal obtained by recrystallization from hexanes was selected and transferred to the goniostat, where it was cooled to −155 °C for characterization and data collection. A systematic search of a limited hemisphere of reciprocal space yielded a set of reflections which exhibited no symmetry or extinctions. The choice of the triclinic space group P1bar was confirmed by successful solution and refinement of the structure.

The structure was solved by a combination of direct methods and heavy-atom Fourier techniques. All non-hydrogen atoms were located and refined by using anisotropic thermal parameters. Hydrogen atoms were included in fixed calculated positions in the final cycles of refinement. The unit cell contains a molecule of *n*-hexane disordered around a center of symmetry (atoms C(40), C(41), C(41′), and C(42)). The solvent atoms were refined by using isotropic thermal parameters. No absorption correction was carried out.

The final difference map was essentially featureless except for a residual of 2 e/Å^3 at the Pt position.

The molecule possesses a crystallographic center of symmetry.

Acknowledgment. We thank the National Science Foundation, the donors of the Petroleum Research Fund, administered by the American Chemical Society, and the Wrubel Computing Center for support. The Varian 300 NMR was purchased in part by a grant (PHS-S10-RR-1882-01) from the National Institutes of Health. Thanks are also extended to the Indiana University NMR Laboratory staff especially for their assistance with ^{183}W NMR. Finally, we acknowledge helpful comments from Professors A. J. Carty of the University of Waterloo and Helmut Werner of the University of Wurzburg.

Supplementary Material Available: Complete listings of bond lengths and bond angles and anisotropic thermal parameters (4 pages); listings of F_o and F_c values (12 pages). Ordering information is given on any current masthead page. The complete structural report is available from the Indiana University Chemistry Library, in microfiche form only. Request MSC Report No. 85074 for Pt[(P(CH$_3$)$_2$C$_6$H$_5$)(C≡C)W$_2$(OC(CH$_3$)$_3$)$_5$]$_2$.

---

[40] Chisholm, M. H.; Huffman, J. C.; Kirkpatrick, C. C. *Inorg. Chem.* **1984**, *23*, 1021.